Chemical Engineering Journal 151 (2009) 188–194

Contents lists available at ScienceDirect

Chemical Engineering Journal

journal homepage: www.elsevier.com/locate/cej

Adsorption of chromium on chitosan: Optimization, kinetics and thermodynamics

Yaşar Andelib Aydın*, Nuran Deveci Aksoy

ITU – Istanbul Technical University, Chemical Engineering Department, Ayazaga Campus, 34469 Istanbul, Turkey

ARTICLE INFO

Article history:
Received 3 December 2008
Received in revised form 10 February 2009
Accepted 11 February 2009

Keywords:
Chromium adsorption
Chitosan
Experimental design
Response surface methodology
Kinetics
Thermodynamics

ABSTRACT

Surface response methodology was involved in the optimization of Cr(VI) adsorption upon chitosan flakes against the process parameters pH, adsorbent dose and initial Cr(VI) concentration. The effects of these factors were studied in the ranges 1.5–9.5, 1.8–24.2 g l^{-1} and 15–95 mg l^{-1}, respectively. A predictive quadratic model was constructed by variance analysis of data obtained from a total of 20 experimental runs with three replicates each. Maximum removal was attained from a solution as concentrated as 30 ppm at pH 3 with an adsorbent dosage of 13 g l^{-1}. The adsorption capacity of chitosan flakes was determined as 22.09 mg g^{-1} at these specified conditions. However, the adsorption capacity was recorded as high as 102 mg g^{-1} for 100 mg l^{-1} initial concentration. Out of Langmuir, Freundlich and Dubinin-Radushkevich isotherm models, adsorption data was best described by Langmuir isotherm with 0.99 consistency. The process kinetics was evaluated by pseudo-first, pseudo-second order and intra-particle diffusion models. Pseudo-second order kinetic model exhibited the highest correlation with data. The results showed that both monolayer adsorption and intra-particle diffusion mechanisms limited the rate of Cr(VI) adsorption. Thermodynamic parameters revealed the feasibility, spontaneity and exothermic nature of adsorption.

1. Introduction

The continuously increasing demand for the commodities produced by chemical industries has triggered heavy metals accumulation in the ecosystem. Being one of the priority pollutants, chromium is discharged to the environment, well above trace limits, as a result of electroplating, leather tanning, cement preservations, paints, pigments, textile, steel fabrication and canning industries [1–3]. There exist three oxidation states for chromium in nature, Cr(II), Cr(III) and Cr(VI), however only the last two of species are stable [4,5]. Cr(VI) is known to be highly mobile in soil and aquatic system, and is also 500 times more toxic, mutagenic and carcinogenic than Cr(III) [2,5]. The maximum permissible limit of for Cr(VI) in wastewater has been recommended as 0.005 mg l^{-1} by World Health Organization [6].

Conventional methods applied for Cr(VI) removal are mainly chemical precipitation, oxidation/reduction, filtration, ion exchange, membrane separation and adsorption [4]. Chemical precipitation produces great amounts of mud, while ion exchangers and membrane separation are relatively of very high cost [7,8]. Therefore, adsorption is the most frequently applied technique owing to its advantages such as variety of adsorbent materials and high efficiency at a relatively lower cost [9]. Although activated carbon is one of the most popular adsorbents for removal of metal ions [4,7,9], current investigations tend towards achieving high removal efficiencies with much cheaper non-conventional materials which are mostly cheap and abundant biological matter [9]. Recently, the removal of metals, compounds, and particulates from solution by biological material is recognized as an extension to adsorption and is named as biosorption [10]. Many biosorbents such as fungi [1], algae [11], seaweeds [12,13], microorganisms [14,15] and several biopolymers [9,16,17] have been utilized in the removal of heavy metals from wastewater.

Chitosan, the major derivative of chitin, and second abundant biopolymer in nature after cellulose, is a good scavenger for metal ions owing to the amine and hydroxyl functional groups in its structure [18–20]. In addition, its adsorption capacity can be improved by chemical means such as crosslinking, addition of functional groups, and by physical conditioning of the biopolymer as gel beads or fibers [20]. The formerly conducted studies considering the adsorption of Cr(VI) have proved that the process parameters, namely, pH, initial concentration, temperature, adsorbent dose and particle diameter influence the removal efficiency immensely [21]. This influence can be realized by inspection of the reported values for Cr(VI) adsorption capacity of chitosan which varies from 27.3 mg g^{-1} [17] to 273 mg g^{-1} [9]. The confusion about adsorption capacity can be overcome by optimization of the parameters involved. Therefore, this study aimed to investigate the effects of process parameters

* Corresponding author. Tel.: +90 2122856878; fax: +90 2122853425.
E-mail address: erdoganyas@itu.edu.tr (Y.A. Aydın).

1385-8947/$ – see front matter © 2009 Elsevier B.V. All rights reserved.
doi:10.1016/j.cej.2009.02.010

on the efficiency of Cr(VI) adsorption by chitosan and to determine the set of parameters leading to maximum removal. The effects of pH, initial concentration and adsorbent dose were studied, while the effects of temperature and particle diameter were excluded intentionally. Surface response methodology was utilized for optimization studies.

Classical methods of optimization involve the change of one variable at a time, which is quite time consuming especially when a large number of variables are considered. Alternatively, response surface methodology aims to optimize the response surface shaped under the influence of the process parameters.

2. Materials and methods

2.1. Reagents

Chitosan flakes (low molecular weight) of deacetylation degree of minimum 85.0% were obtained from Sigma–Aldrich (Missouri, USA). The flakes with average particle size of 1300 μm were used in experiments without further pretreatment. Extra pure potassium dichromate, 37.0% pure HCl, and analysis grade 1,5-diphenyl carbazide were purchased from Merck (Darmstadt, Germany). Sodium hydroxide (≥98.0%), nitric acid (65.0%), and sulphuric acid (95–97%) were obtained from Fluka (Buchs, Switzerland). Acetone (99.0%) used in preparation of 1,5-diphenyl carbazide solution was purchased from Carlo Erba (Rodano, Italy). Deionized water was involved in preparation of all solutions as well as rinsing of glassware.

2.2. Design of experiments

Central composite design was employed in the experimental design procedure. The total number and sequence of experimental runs were determined using MINITAB for windows Release 15 software (MINITAB Inc., Pennsylvania, USA). According to this design, 20 experiments were conducted with three replications each to ensure the accuracy of the results. The effects of process parameters pH, ion concentration and adsorbent dosage were investigated at five levels as summarized in Table 1. Significance level (α) was chosen as 0.05.

Surface plots were constructed by MINITAB. Main effects and interactions of the factors were determined by fitting a second order polynomial equation (Eq. (1)) and by interpretation of the ANOVA table. A variable was considered significant when the calculated probability value (p) was smaller than the chosen significance level. In case of insignificance the variable was omitted from the predictive model (Eq. (1)).

$$y = \beta_0 + \sum_{i}^{k} \beta_i x_i + \sum_{i}^{k} \beta_{ii} x_i^2 + \sum_{i} \sum_{j} \beta_{ij} x_i x_j + \varepsilon_r \quad (1)$$

Here, y is the predicted response, i and j take value from 1 to the number of independent process variables. The β values are coefficients predicted by the method of least squares, ε_r is the error of prediction and x_i and x_j are the level of the independent process variables [22–24]. The response surface plots constructed by the aid of predictive model were used in determination of the optimum values of the process variables leading to maximum removal percentage.

Table 1
Lower and upper bounds of the parameters.

Parameters	Coded value				
	−1.6	−1	0	1	1.6
pH	1.5	3	5.5	8	9.5
Initial concentration (mg l^{-1})	15	30	55	80	95
Adsorbent dose (g l^{-1})	1.8	6	13	20	24.2

2.3. Adsorption experiments

Stock Cr(VI) solution of 500 ppm was prepared using $K_2Cr_2O_7$ with deionized water. For further experiments, solutions of 50 ml volume were prepared by dilution of this stock. Batch tests were conducted in 100 ml stoppered flasks in a water bath kept at 298 K. Agitation rate was held constant at 120 rpm. The pH of the solutions was regulated by micro-additions of 0.2N H_2SO_4 and 0.1N NaOH. Isotherm data were obtained by placing 5 g l^{-1} flakes in chromium solutions of different initial concentration (5–200 mg l^{-1}). Experiments were performed at 303.15–333.15 K for evaluation of thermodynamic parameters. Concentration was monitored with respect to time for kinetic analysis. The concentration of the samples was analyzed spectrophotometrically (Shimadzu UV 1240) at 540 nm using 1,5-diphenyl carbazide as the complexing agent [4–6].

3. Results and discussion

3.1. Data analysis and construction of model

The sequence of experiments and summary of the results are given in Table 2. The removal percentages listed in the fifth column represent the average result of three parallel experiments and they were calculated according to Eq. (2).

$$\text{Removal\%} = \frac{C_0 - C_e}{C_0} \times 100 \quad (2)$$

where C_0 and C_e are the initial and equilibrium concentration of solutions (mg l^{-1}), respectively. Removal percentage values were recorded as the response of the system and the values were used in creating the surface plots shown in Figs. 1–3.

Variance analysis conducted for full quadratic model including all linear, square and interaction terms proved that the interaction and square terms other than the square effect of pH had very poor effect on the adsorption of Cr(VI). Although the regression coefficient of this model was quite high (0.93), a large difference was observed with the adjusted regression coefficient (0.86). When insignificant terms were excluded from the model, the regression coefficient happened to drop to 0.90; however, adjusted regres-

Table 2
Calculated results for adsorption of Cr(VI) on chitosan.

Experiment no.	Initial concentration	Adsorbent dose	pH	Removal (%)
1	−1.0	−1.0	−1.0	84.18
2	1.6	0.0	0.0	88.47
3	0.0	1.6	0.0	78.42
4	0.0	0.0	0.0	93.12
5	0.0	0.0	0.0	76.89
6	0.0	0.0	0.0	93.36
7	0.0	0.0	1.6	84.71
8	−1.6	0.0	0.0	59.99
9	0.0	0.0	−1.6	85.52
10	−1.0	1.0	−1.0	72.38
11	1.0	1.0	1.0	84.98
12	−1.0	−1.0	1.0	64.42
13	0.0	−1.6	0.0	96.07
14	0.0	0.0	0.0	80.69
15	0.0	0.0	0.0	59.77
16	1.0	1.0	−1.0	92.81
17	−1.0	1.0	1.0	96.56
18	1.0	−1.0	1.0	82.84
19	1.0	−1.0	−1.0	64.11
20	0.0	0.0	0.0	82.03

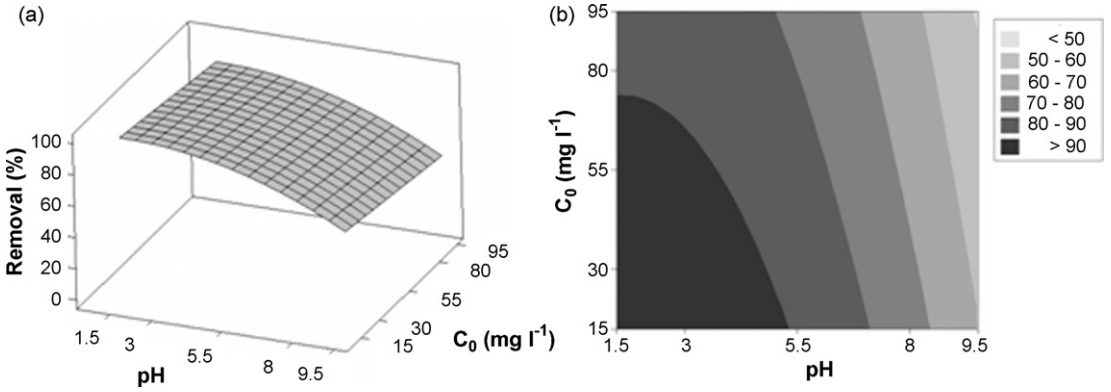

Fig. 1. (a) Surface, (b) contour plot for pH-initial concentration pair (ads. dose = 13 g l^{-1}).

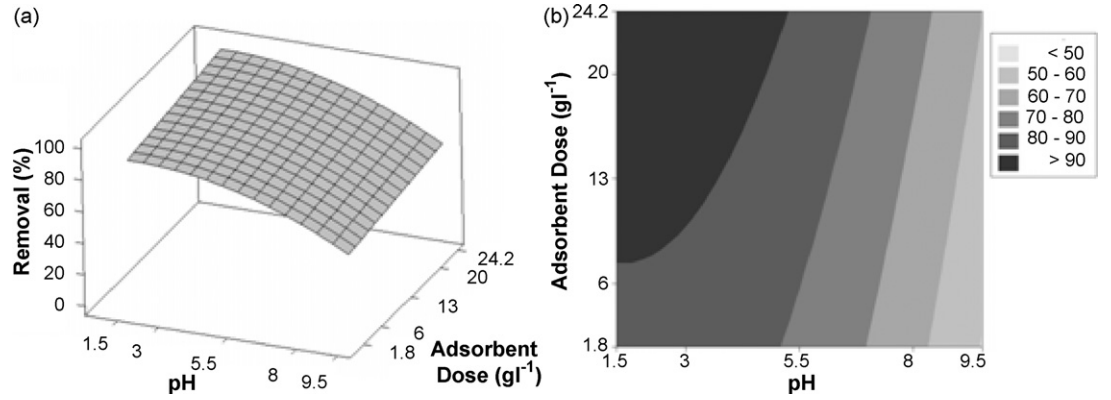

Fig. 2. (a) Surface, (b) contour plot for pH-adsorbent dose pair (C_0 = 55 mg l^{-1}).

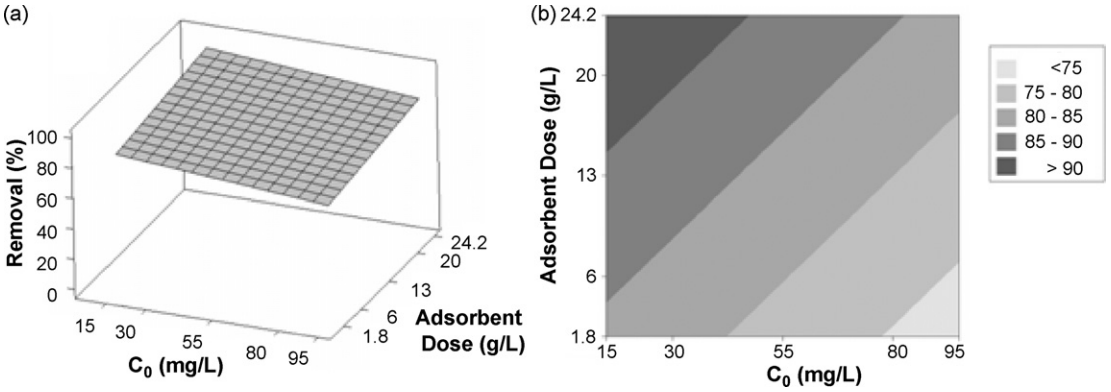

Fig. 3. (a) Surface, (b) contour plot for initial concentration-adsorbent dose pair (pH 5.5).

sion coefficient increased to 0.87. Both the narrowed gap between the regression coefficients and the decreased standard deviation were accepted as indications of enhanced strength of the model. The ANOVA table for the final model given in Eq. (3) is provided in Table 3.

$$\text{Removal}\ (\%) = 83.555 - 11.783 \times \text{pH} - 3.55 \times C_0 + 3.353 \times \text{adsorbent dose} - 3.795 \times \text{pH}^2 \qquad (3)$$

The outcomes of variance analysis were used to evaluate the intensity of the effects of process conditions. The probability values were calculated as 0.000, 0.008, and 0.011 for pH, initial concentration and adsorbent dosage, respectively. Since all p values were lower than significance level, all parameters were effective on the extent of adsorption at main effect levels. However, the order of significance for main effects was determined as pH > initial concentration > adsorbent dose.

Table 3
Analysis of variance for the final model.

Source	DF	Seq SS	Adj SS	Adj MS	*F*	*P*
Regression	4	2314.31	2314.31	578.578	32.80	0.000
Linear	3	2134.32	2134.32	711.441	40.33	0.000
Square	1	179.99	179.99	179.988	10.20	0.006
Residual Error	15	264.61	264.61	17.640	8.82	0.013
Lack-of-Fit	10	250.41	250.41	25.041		
Pure Error	5	14.20	14.20	2.840		
Total	19	2578.92				

3.2. Surface and contour plots

Surface and contour plots were used in determination of the optimum set of process conditions. The surfaces constructed under the combined effect of process parameters are shown in Figs. 1–3.

3.2.1. The pH effect

Figs. 1 and 2 show the combined effect of pH with initial concentration and adsorbent dose, respectively. The effect of pH was found to be the highest amongst studied variables. A major drop was observed in removal extent as pH was increased from 1.5 to 9.5 in both figures. Accordingly, when pH was held in the strongly acidic region, preferably below pH 3, over 90% removal was attained regardless of initial concentration and adsorbent dose. Cr(VI) exists predominantly as $HCrO_4^-$ in aqueous solution below pH 4. Since the amino groups of chitosan are protonated at this pH, electrostatic interaction occurs between the sorbent and $HCrO_4^-$ ions [3,25] resulting in high chromium removal. Previous works by Hamadi et al. [3], Karthiyekan et al. [8], Qin et al. [25] and Sari and Tuzen [26] have also presented 95, 81, 96 and 85% Cr(VI) removal, respectively, under similar pH conditions for various adsorbents.

3.2.2. The effect of initial concentration

The combined effects of initial concentration with pH and adsorbent dose are visualized in Figs. 1 and 3. Initial concentration implied a considerable effect on Cr(VI) removal. The extent of removal was suppressed by approximately 15% when initial concentration was increased from 15 to 95 mg l^{-1} for constant pH and adsorbent dose levels. On the contrary, the adsorption capacity of chitosan was calculated to increase from 2.9 to 102 mg g^{-1} with rise in initial concentration from 5 to 100 mg l^{-1}. This can mainly be attributed to the increase in concentration gradient in the system which results with enhanced efficiency of Cr(VI) adsorption.

3.2.3. The effect of adsorbent dose

Figs. 2 and 3 show the effect of adsorbent dose on removal percentage. Accordingly, when pH was held below pH 3, an adsorbent dose of 7 g l^{-1} was sufficient to ensure >90% Cr(VI) removal for solutions up to 55 mg l^{-1} initial concentration. For lower initial concentrations, even 1.8 g l^{-1} was efficient at significantly acidic pH. Although both plots exhibited enhanced Cr(VI) removal at higher adsorbent doses, the improvement of removal percentage was not sufficient to justify the excessive use of adsorbent and the related costs. The general range for dosage of conventional adsorbents is reported as 1–20 g l^{-1} in literature [9], thus chitosan exhibited high efficacy for Cr(VI) adsorption.

3.2.4. Optimum set of process variables

The optimum levels of factors were predicted as pH 3, initial concentration of 30 mg l^{-1} and 24.2 g l^{-1} adsorbent dose by the model. At those conditions, the model predicted 100% Cr(VI) removal. Experiments were conducted to check the accuracy of the optimum set of parameters and the resulting removal percentage was compared to the output of the model. Experimental results showed that only 89.2% removal could be attained at those conditions. Further experiments proved that the optimum adsorbent dose was 13 g l^{-1}, by which 92.9% Cr(VI) removal was achieved.

3.3. Equilibrium isotherms

The relationship between adsorbed metal concentration and concentration of the solution at equilibrium is described by isotherm models, of which Langmuir and Freundlich are the most widely referred equations. Langmuir isotherm model, given in Eq. (4), is representative of monolayer adsorption occurring on an energetically uniform surface on which the adsorbed molecules are not interactive [19,27]. Accordingly, equilibrium is attained once the monolayer is completely saturated [2]. The non-linear model is transformed into Eq. (5) so that the corresponding constants can be computed.

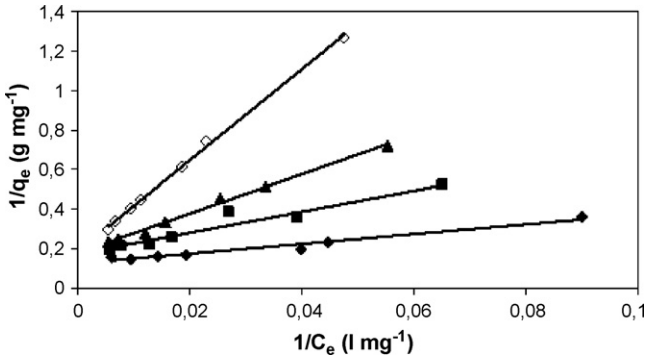

Fig. 4. Langmuir plot for adsorption of Cr(VI) upon chitosan. (♦) 303.15 K, (■) 313.15 K, (▲) 323.15 K, (◊) 333.15 K; pH 4.

$$q_e = \frac{q_m b C_e}{1 + bC_e} \tag{4}$$

$$\frac{1}{q_e} = \frac{1}{q_m} + \frac{1}{bq_m C_e} \tag{5}$$

Here, q_e is the equilibrium adsorption capacity (mg g^{-1}), C_e is the equilibrium concentration of solution (mg l^{-1}), q_m is the Langmuir constant representing the maximum adsorption capacity (mg g^{-1}) and b is the Langmuir constant related to the energy of adsorption (l^{-1} mg). The values of Langmuir constants q_m and b were obtained from the intercept and slope of the plot between $(1/q_e)$ vs. $(1/C_e)$ presented in Fig. 4. The computed constants are shown in Table 4. The experimental data exhibited high correlation with Langmuir model within the studied temperature range. Both q_m and b decreased in the order of increasing temperature. While this outcome is contradictory to some of the studies involving Cr(VI) adsorption on various materials such as humic acids [28], sawdust activated carbon [8] magnesia cement [29], groundnut husk carbon [2], Sharma and Weng [30] have reported decreasing Langmuir constants with temperature for adsorption of Cr(VI) on riverbed sand which is an indication that the behavior is adsorbent specific.

Contradictory to Langmuir, Freundlich model, shown in Eq. (6), describes the adsorption on an energetically heterogeneous surface on which the adsorbed molecules are interactive [2,27,30]. The model is linearized to give Eq. (7):

$$q_e = K_F C_e^{1/n} \tag{6}$$

$$\ln\ q_e = \ln K_F + \frac{1}{n} \ln C_e \tag{7}$$

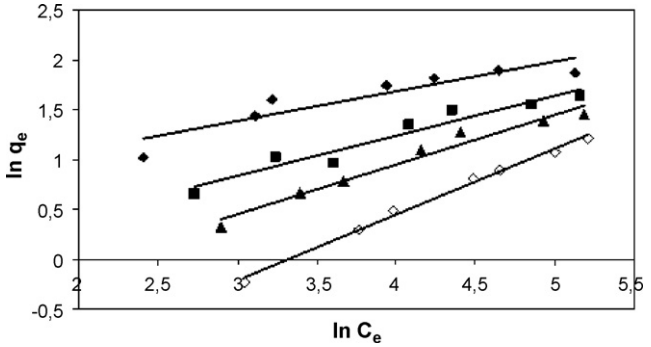

Fig. 5. Freundlich plot for adsorption of Cr(VI) upon chitosan. (♦) 303.15 K, (■) 313.15 K, (▲) 323.15 K, (◊) 333.15 K; pH 4.

Table 4
Isotherm constants for Cr(VI) adsorption upon chitosan.

Temperature (K)	Langmuir				Freundlich		
	q_m (mg g^{-1})	b (l mg^{-1})	R_L	R^2	K_F (mg g^{-1})	n	R^2
303.15	7.943	0.050	0.444	0.971	1.616	3.328	0.835
313.15	5.774	0.032	0.555	0.934	0.685	2.480	0.931
323.15	5.663	0.018	0.689	0.995	0.351	2.003	0.968
333.15	5.246	0.008	0.833	0.998	0.111	1.513	0.994

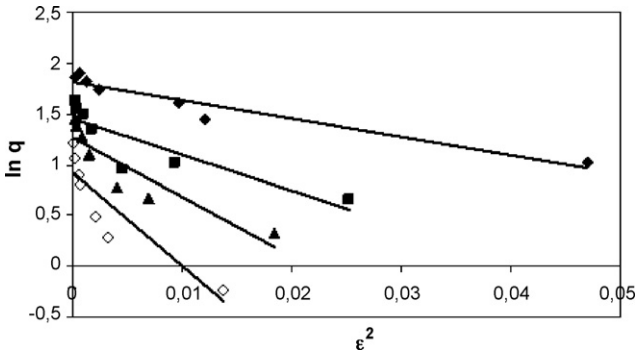

Fig. 6. Dubinin-Radushkevich plot for adsorption of Cr(VI) upon chitosan. (♦) 303.15 K, (■) 313.15 K, (▲) 323.15 K, (◊) 333.15 K; pH 4.

where K_F and n are constants for Freundlich isotherm that are indicative of the adsorption capacity (mg g^{-1}) and intensity of the adsorbent, respectively [2,28]. The values of K_F and n were calculated from the slope and intercept of the plot between $\ln q_e$ and $\ln C_e$ (Fig. 5). The calculated constants are reported in Table 4. All constants exhibited significant decrement with rise in temperature, which is an indication of the exothermic nature of the process. Inspection of the regression coefficients proved that the correlation of Langmuir model was stronger with respect to Freundlich model for temperatures studied.

The experimental data was fitted to Dubinin-Radushkevich isotherm model in order to determine the adsorption type. The non-linear model given with Eq. (8) is reduced to linear form as in Eq. (9).

$$q_e = q_m \exp(-k\varepsilon^2) \tag{8}$$

$$\ln q_e = \ln q_m - k\varepsilon^2 \tag{9}$$

where q_m is the maximum adsorption capacity (mg g^{-1}), k is a constant related to the energy of adsorption (mol^2 kJ^{-2}) and ε is the Polanyi potential, which is calculated from Eq. (10) [5,31,32].

$$\varepsilon = RT \ln\left(1 + \frac{1}{C_e}\right) \tag{10}$$

where R is the universal gas constant (kJ mol^{-1} K^{-1}) and T is temperature (K). The isotherm constants q_m and k were calculated from the slope and intercept of the plot of $\ln q_e$ vs. ε^2 (Fig. 6). As observed from the figure, the data were not consistent with the model for temperatures higher than 303.15 K, i.e. $R^2 < 0.8$. The value of k was calculated as 17.953 mol^2 kJ^{-2} for 303.15 K. The mean free energy of adsorption (E) was calculated using the value of k according to Eq. (11).

$$E = (2k)^{-0.5} \tag{11}$$

Accordingly, the value of E is 0.167 kJ mol^{-1}. The common regard about E is that it depicts adsorption by ion exchange when its value is between 8 and 16 kJ mol^{-1} [5]. The value of E calculated in this study is substantially lower than 8 kJ mol^{-1} indicating that the adsorption of Cr(VI) on chitosan occurs via physical adsorption due to weak van der Waals forces [26,27,31].

A dimensionless separation factor (R_L) was calculated by Eq. (12) for confirmation of the efficiency of adsorption.

$$R_L = \frac{1}{(1 + bC_0)} \tag{12}$$

where b is the Langmuir constant (l mg^{-1}) and C_0 is the initial adsorbate concentration (mg l^{-1}). While $0 < R_L < 1$ denotes favorable adsorption, $R_L > 1$ is an indication of unfavorable adsorption [5,33]. The values for R_L listed in Table 4 were calculated for 25 mg l^{-1} initial concentration, which is the lowest initial Cr(VI) concentration, applied for isotherm studies. The values of R_L are all in the range 0–1, which indicates the favorability of Cr(VI) adsorption by chitosan.

3.4. Kinetic analysis

Kinetic analysis is required to get an insight of the rate of adsorption and the rate limiting step of the transport mechanism, which are primarily used in the modeling, and design of the process [3]. Collected data (not shown) proved that majority of Cr(VI) molecules present in solution were adsorbed very rapidly within the first hour while equilibrium was attained at the end of third hour for the highest initial concentration studied (100 mg g^{-1}). The experimental data was fitted with linearized forms of pseudo-first order (Eq. (13)), pseudo-second order (Eq. (14)) [3,13,27–30], Elovich (Eq. (15)) [30] and intra-particle diffusion (Eq. (16)) [8,27,33] model equations.

$$\log(q_e - q_t) = \log\ q_e - \frac{k_1}{2.303}t \tag{13}$$

$$\frac{t}{q_t} = \frac{1}{k_2 q_e^2} + \frac{1}{q_e}t \tag{14}$$

$$q_t = \frac{1}{\beta}\ln(\alpha\beta) + \frac{1}{\beta}\ln t \tag{15}$$

$$q_t = Kt^{0.5} \tag{16}$$

where k_1 (h^{-1}) and k_2 (mg g^{-1} h^{-1}) are rate constants of adsorption, q_e (mg g^{-1}) is the equilibrium adsorption capacity, q_t (mg g^{-1}) is the adsorption at any time t (h), α is the initial adsorption

Table 5
Kinetic parameters for Lagergren and Elovich models.

C_0 (mg l^{-1})	Pseudo-first order			Pseudo-second order			Elovich model		
	k_1 (h^{-1})	q_e (mg g^{-1})	R^2	k_2 (g mg^{-1} h^{-1})	q_e (mg g^{-1})	R^2	B (g mg^{-1})	$\alpha \times 10^3$ (mg g^{-1} h^{-1})	R^2
5	0.999	0.866	0.890	3.103	3.583	0.999	2.624	1.383	0.894
25	1.205	18.209	0.971	0.151	34.722	0.999	0.194	1.026	0.948
100	1.140	29.874	0.962	0.120	102.041	1.000	0.137	2.041	0.963

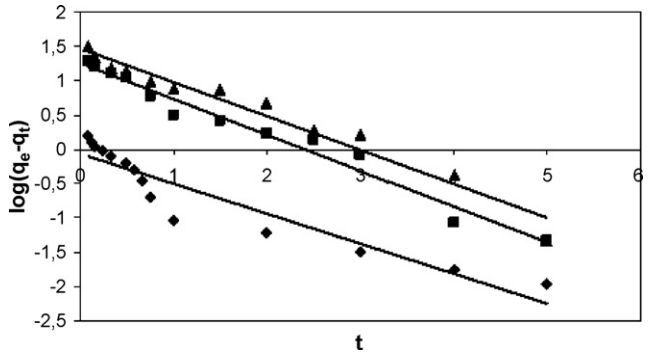

Fig. 7. Plot for first order kinetics, C_0 (mg l^{-1}): (♦) 5, (■) 25, (▲) 100; pH 4; T: 293.15 K.

rate (mg g^{-1} h^{-1}), β is the desorption constant (g mg^{-1}) and K is the intra-particle diffusion constant (mg g^{-1} h$^{-0.5}$). All the kinetic parameters other than K have been postulated from the slopes and the intercepts of respective plots (Figs. 7–9) and are summarized in Table 5. The results of the regression analysis proved that Cr(VI) adsorption on chitosan was best described by the pseudo-second order equation ($R^2 \approx 1.000$) for all three of studied concentrations. The equilibrium capacities calculated from pseudo-second order model agreed closely with the capacities found from isotherm studies. Some very recent investigations concerning the kinetics of Cr(VI) adsorption onto various adsorbents have also reported higher correlations for pseudo-second order model [3,8,13,25,28,33]. The decrease in adsorption rate with increase in initial concentration is quite straightforward due to the increase in driving force for mass transfer [33].

The intra-particle diffusion constant was computed from the plot of q_t vs. $t^{0.5}$. All plots in Fig. 10 present two separate regions with different slopes. This is an indication of multistep limited

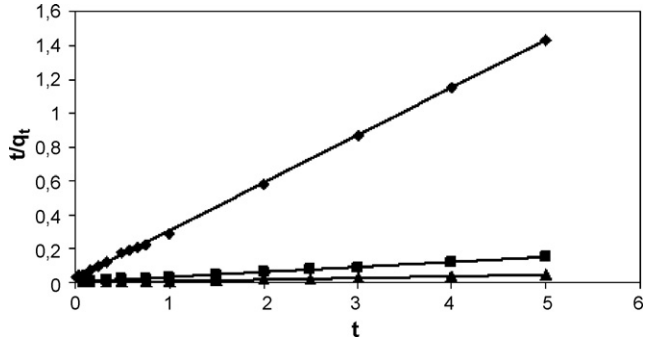

Fig. 8. Plot for second order kinetics, C_0 (mg l^{-1}): (♦) 5, (■) 25, (▲) 100; pH 4; T: 293.15 K.

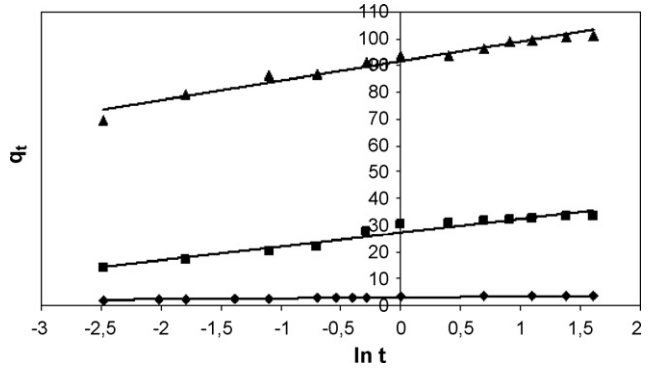

Fig. 9. Plot for Elovich model, C_0 (mg l^{-1}): (♦) 5, (■) 25, (▲) 100; pH 4; T: 293.15 K.

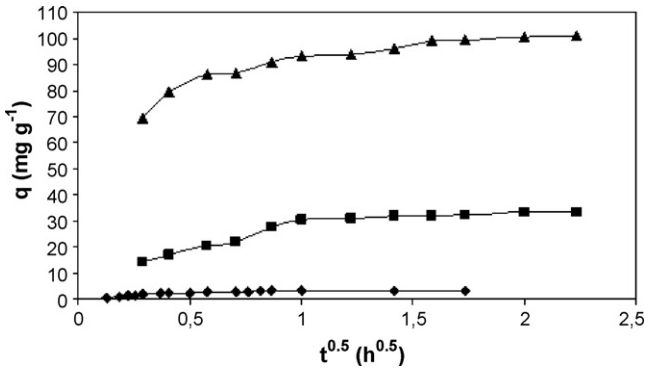

Fig. 10. Plot for intra-particle diffusion model, C_0 (mg l^{-1}): (♦) 5, (■) 25, (▲) 100; pH 4; T: 293.15 K.

adsorption process. The curved region of plot reflects boundary layer diffusion while the linear portion stands for intra-particle diffusion [8,27,33]. The intra-particle diffusion constants calculated from the slope of the linear region were 7.879, 22.451 and 34.777 mg g^{-1} h$^{-0.5}$ at 5, 25 and 100 mg g^{-1} initial Cr(VI) concentration, respectively.

3.5. Thermodynamics

The decrease in adsorption capacity with rise in temperature (Table 4) was attributed to the exothermic nature of the process and was further explained by evaluation of thermodynamic parameters [3,8]. The Gibb's free energy change (ΔG°) can be evaluated from Eq. (17):

$$\Delta G^\circ = -RT \ln k_0 \quad (17)$$

where R is the universal gas constant (kJ mol^{-1} K^{-1}), T is temperature (K) and k_0 is the equilibrium constant (m^3 mol^{-1}) [21]. The Gibbs free energy change is also related to enthalpy change (ΔH°) and entropy change (ΔS°) at constant temperature by Eq. (18) [15,27]:

$$\ln k_0 = \frac{\Delta S^\circ}{R} - \frac{\Delta H^\circ}{RT} \quad (18)$$

The values of ΔH° and ΔS° were calculated from the slope and intercept of the Van't Hoff plot ($\ln k_0$ vs. $1/T$) shown in Fig. 11 [5]. The calculated values are given in Table 6. The Gibbs free energy change (ΔG°) values were found to be negative below 313.15 K, which indicated the feasibility and spontaneity of the adsorption at temperatures below 313.15 K. The enthalpy change was −50.782 kJ mol^{-1}, which indicated the exothermic nature of adsorption process. The negative entropy change (ΔS°) for the

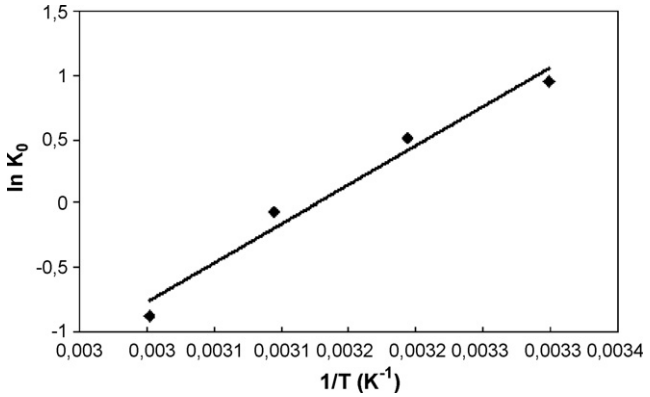

Fig. 11. Van't Hoff plot for estimation of thermodynamic parameters.

Table 6
Thermodynamic parameters for Cr(VI) adsorption on chitosan.

Temperature (K)	K_0 ($m^3\ mol^{-1}$)	ΔG° ($kJ\ mol^{-1}$)	ΔH° ($kJ\ mol^{-1}$)	ΔS° ($kJ\ mol^{-1}\ K^{-1}$)
303.15	2.601	−2.409	−50.782	−0.159
313.15	1.664	−1.326		
323.15	0.936	0.178		
333.15	0.416	2.429		

process was caused by the decrease in degree of freedom of the adsorbed species [21,26,29].

4. Conclusions

Chitosan, a polymer of biological origin, has been reported to be an effective adsorbent for Cr(VI) removal from wastewater [17–19,21,25,31,34], however several different values have been determined for adsorption capacity and optimum process conditions. Since the cost of chitosan is considerably high, optimization is essential for efficient use of material. In this study, Cr(VI) removal ratio was optimized by surface response methodology. Accordingly, a maximum of 92.9% Cr(VI) removal was attained at pH 3 with $13\ g\ l^{-1}$ chitosan flakes from a solution initially concentrated as $30\ mg\ l^{-1}$. While the adsorption capacity of chitosan was calculated as $22.09\ mg\ g^{-1}$ at those conditions, the adsorption capacity was calculated as high as $102\ mg\ g^{-1}$ for $100\ mg\ l^{-1}$ initial Cr(VI) concentration which is remarkably higher than $76\ mg\ g^{-1}$ as reported by Schmuhl et al. [34] at similar experimental conditions. pH was determined to be the most effective parameter, followed with initial concentration and adsorbent dose. The Langmuir isotherm model provided the best fit for experimental data which indicated monolayer adsorption. Kinetic parameters showed that the adsorption of Cr(VI) on chitosan was described best by pseudo-second order model while both boundary layer and intra-particle diffusion steps contributed to the rate of process. The mean free energy of adsorption (E) was calculated as $0.167\ kJ\ mol^{-1}$ proving physical adsorption occurring due to weak van der Waals forces. Thermodynamic analysis confirmed the spontaneous and exothermic character of adsorption process. The decrease in randomness of species resulted with negative ΔS°.

References

[1] R.I. Acosta, X. Rodriguez, C. Gutierrez, G. Moctezuma, Biosorption of chromium (VI) from aqueous solutions onto fungal biomass, Bioinorg. Chem. Appl. 2 (1–2) (2004) 1–7.
[2] S.P. Dubey, K. Gopal, Adsorption of chromium (VI) on low cost adsorbents derived from agricultural waste material: a comparative study, J. Hazard. Mater. 145 (2007) 465–470.
[3] N.K. Hamadi, X.D. Chena, M.M. Farid, M.G.Q. Lub, Adsorption kinetics for the removal of chromium (VI) from aqueous solution by adsorbents derived from used tyres and sawdust, Chem. Eng. J. 84 (2001) 95–105.
[4] D. Mohan, C.U. Pittman Jr., Activated carbons and low cost adsorbents for remediation of tri- and hexavalent chromium from water, J. Hazard. Mater. B137 (2006) 762–811.
[5] V. Sarin, K.K. Pant, Removal of chromium from industrial waste by using eucalyptus bark, Bioresour. Technol. 97 (2006) 15–20.
[6] C.A. Kozlowski, W. Walkowiak, Removal of chromium (VI) from aqueous solutions by polymer inclusion membranes, Water Res. 36 (2002) 4870–4876.
[7] S.M. Nomanbhay, K. Palanisamy, Removal of heavy metal from industrial wastewater using chitosan coated oil palm shell charcoal, Elect. J. Biotechnol. 8 (2005) 43–53.
[8] T. Karthikeyan, S. Rajgopal, L.M. Miranda, Chromium (VI) adsorption from aqueous solution by *Hevea Brasilinesis* sawdust activated carbon, J. Hazard. Mater. B124 (2005) 192–199.
[9] S. Babel, T.A. Kurniawan, Low-cost adsorbents for heavy metals uptake from contaminated water: a review, J. Hazard. Mater. B97 (2003) 219–243.
[10] V. Boddu, K. Abburi, J.L. Talbott, E.D. Smith, Removal of hexavalent chromium from wastewater using a new composite chitosan biosorbent, Environ. Sci. Technol. 37 (2003) 4449–4456.
[11] V.K. Gupta, A.K. Shrivastava, N. Jain, Biosorption of chromium (VI) from aqueous solution by green algae *Spirogyra* species, Water Res. 35 (2001) 4079–4085.
[12] D. Kratochvil, P. Pimentel, B. Volesky, Removal of trivalent and hexavalent chromium by seaweed biosorbent, Environ. Sci. Technol. 32 (1998) 2693–2698.
[13] R. Elangovan, L. Philip, K. Chandraraj, Biosorption of chromium species by aquatic weeds: kinetics and mechanism studies, J. Hazard. Mater. 152 (2008) 100–112.
[14] Y. Sahin, A. Ozturk, Biosorption of chromium (VI) ions from aqueous solution by the bacterium *Bacillus thuringiensis*, Process Biochem. 40 (2005) 1895–1901.
[15] T. Fan, Y. Liu, B. Feng, G. Zeng, C. Yang, M. Zhou, H. Zhou, Z. Tan, X. Wang, Biosorption of cadmium (II), zinc (II) and lead (II) by *Penicillium simplicissimum*: isotherms, kinetics and thermodynamics, J. Hazard. Mater. 160 (2008) 655–661.
[16] Y. Wu, S. Zhang, X. Guo, H. Huang, Adsorption of chromium(III) on lignin, Bioresour. Technol. 99 (2008) 7709–7715.
[17] S.E. Bailey, T.J. Olin, R.M. Bricka, D.D. Adrian, A review of potentially low-cost sorbents for heavy metals, Water Res. 33 (1999) 2469–2479.
[18] F. Zhao, Y. Binyu, Z. Yue, T. Wang, X. Wen, Z. Liu, C. Zhao, Preparation of porous chitosan gel beads for copper(II) ion adsorption, J. Hazard. Mater. 147 (2007) 67–73.
[19] P. Baroni, R.S. Vieira, E. Meneghetti, M.G.C. da Silva, M.M. Beppu, Evaluation of batch adsorption of chromium ions on natural and crosslinked chitosan membranes, J. Hazard. Mater. 152 (2008) 1155–1163.
[20] N.M. Alves, J.F. Mano, Chitosan derivatives obtained by chemical modifications for biomedical and environmental applications, Int. J. Biol. Macromol. 43 (2008) 401–414.
[21] G. Rojas, J. Silva, J.A. Flores, A. Rodriguez, Adsorption of chromium onto cross-linked chitosan, Sep. Purif. Technol. 44 (2005) 31–36.
[22] K. Palanikumar, R. Karthikeyan, Optimal machining conditions for turning of particulate metal matrix composites using Taguchi and response surface methodologies, Mach. Sci. Technol. 10 (2006) 417–433.
[23] Z. Xiong, X. Tu, G. Tu, Optimization of medium composition for actinomycin X2 production by *Streptomyces* spp. JAU4234 using response surface methodology, J. Ind. Microbiol. Biotechnol. 35 (2008) 729–734.
[24] Md. Altaf, M. Venkateshwar, M. Srijana, G. Reddy, An economic approach for L-(+) lactic acid fermentation by *Lactobacillus amylophilus* GV6 using inexpensive carbon and nitrogen sources, J. Appl. Microbiol. 103 (2007) 372–380.
[25] C. Qin, Y. Du, Z. Zhang, Y. Liu, L. Xiao, X. Shi, Adsorption of chromium (VI) on a novel quaternized chitosan resin, J. Appl. Polym. Sci. 90 (2003) 505–510.
[26] A. Sari, M. Tuzen, Removal of Cr(VI) from aqueous solution by Turkish vermiculite: equilibrium, thermodynamic and kinetic studies, Sep. Sci. Technol. 43 (2008) 3563–3581.
[27] T.S. Singh, K.K. Pant, Equilibrium, kinetics and thermodynamic studies for adsorption of As(III) on activated alumina, Sep. Purif. Technol. 36 (2004) 139–147.
[28] L. Ying, Y. Qinyan, G. Baoyu, L. Qian, L. Chunling, Adsorption thermodynamic and kinetic studies of dissolved chromium onto humic acids, Colloids Surf. B 65 (2008) 25–29.
[29] M.S. Gasser, G.H.A. Morad, H.F. Aly, Batch kinetics and thermodynamics of chromium ions removal from waste solutions using synthetic adsorbents, J. Hazard. Mater. 142 (2007) 118–129.
[30] Y.C. Sharma, C.H. Weng, Removal of chromium(VI) from water and wastewater by using riverbed sand: kinetic and equilibrium studies, J. Hazard. Mater. 142 (2007) 449–454.
[31] S.P. Ramnani, S. Sabharwal, Adsorption behavior of Cr(VI) onto radiation crosslinked chitosan and its possible application for the treatment of wastewater containing Cr(VI), React. Funct. Polym. 66 (2006) 902–909.
[32] C. Quintelas, B. Fernandes, J. Castro, H. Figueiredo, T. Tavares, Biosorption of Cr(VI) by a *Bacillus coagulans* biofilm supported on granular activated carbon (GAC), Chem. Eng. J. 136 (2008) 195–203.
[33] S. Debnath, U.C. Ghosh, Kinetics, isotherm and thermodynamics for Cr(III) and Cr(VI) adsorption from aqueous solutions by crystalline hydrous titanium oxide, J. Chem. Thermodyn. 40 (2008) 67–77.
[34] R. Schmuhl, H.M. Krieg, K.A. Keizer, Adsorption of Cu(II) and Cr(VI) ions by chitosan: kinetics and equilibrium studies, Water S.A. 27 (2001) 1–7.